Journal of Energy Storage 55 (2022) 105647

Contents lists available at ScienceDirect

Journal of Energy Storage

journal homepage: www.elsevier.com/locate/est

Research Papers

Improving the drum solar still performance using corrugated drum and nano-based phase change material

Amer A. Saeed [a], Abdulaziz M. Alharthi [a], Khaled M. Aldosari [a], A.S. Abdullah [a,b,*], Fadl A. Essa [c], Umar F. Alqsair [a], Mutabe Aljaghtham [a], Z.M. Omara [c]

[a] Department of Mechanical Engineering, College of Engineering in Al-Kharj, Prince Sattam bin Abdulaziz University, Al-Kharj, 11942, Saudi Arabia.
[b] Tanta University, Faculty of Engineering, Department of Mechanical Power Engineering, Tanta 31521, Egypt
[c] Kafrelsheikh University, Faculty of Engineering, Department of Mechanical Engineering, Kafrelsheikh 33516, Egypt

ARTICLE INFO

Keywords:
Phase change material
Ag nanoparticle
Drum solar still
Solar still
Speed
Corrugated drum

ABSTRACT

The problem of lack of safe drinking water is one of the problems that trouble governments all over the world. There are many methods of desalinating sea water, including solar distillers, which are used to contribute to solving this problem in places far from urbanization and not supplied with traditional energy sources and where there is an abundance of solar energy. In this work, a new design of drum solar still (DSS) was proposed to improve its productivity. The proposed design included a corrugated drum solar still (CDSS), conventional drum solar still (DSS), and conventional solar still (CSS). The DSS contained a rotating flat drum, and CDSS contained a rotating corrugated drum. These drums were operated by a DC motor connected to photovoltaic panels. In addition, the impact of using nano-painting for the CDSS and phase change material (PCM) mixed with Ag nanomaterial was tested on the CDSS performance. Besides, the effect of rotating the drum at various speeds (0.05, 0.1, 0.3, 0.5, 0.7 rpm) was tested. Additionally, environmental and economic analyses were carried out to make sure the reliability of the performance of the tested system. The experimental results showed that the yield was improved by 318 % for CDSS with corrugated drum, Ag-black paint and PCM-Ag at 0.1 rpm compared to that of CSS. In addition, the CDSS is capable to mitigate 14 tons of CO_2 per year. The costs of 1 L from the CDSS and CSS were 0.039 and 0.048$, respectively.

1. Introduction

Scientists were urged to come up with novel desalination concepts and technologies for extracting freshwater from salt water to overcome the potable water shortage crisis in the arid area. Due to its numerous advantages, solar water distillation utilizing solar stills is a traditional method for desalination of salt water. However, it suffers from the low freshwater productivity [1,2]. Because the solar still has low daily production, many investigations have been performed to maximize the freshwater production of solar stills such as increasing the temperature of feed water by using solar water collectors [3–5]. These investigations focused on minimizing the saline water depth in solar stills [6,7] and employing mirrors to increase the incident solar energy to the solar still [8,9]. In addition, several publications connected the artificial intelligence (AI) with the renewable energy-based devices and materials [10–13]. References [14–17] used the artificial neural networks (ANNs) to predict the thermal performance of solar stills under various operating conditions. It was reported that these ANN predicting techniques have good and optimized tools for the performance prediction. Several studies have been accomplished to improve the freshwater production of the solar distillers [18–20]. The modifications include using pyramid solar stills [21–23], hemispherical solar stills [24], the wick, finned and corrugated solar distillers [25–28], stepped stills [29–32], rotating parts to enlarge the area of evaporation and to break the surface tension of saline water of stills [33–35], blades solar stills [36–38], convex solar stills [39–41], nanofluids solar distillers [42–45], tubular drum solar distillers [46,47], disc distillers [48,49], rotating wick distillers [50–52], rotating-drum solar distillers [53,54], and trays solar stills [55–58].

The free surface area of condensation and evaporation is one of the most important elements impacting freshwater output of a solar still [59]. As a result, a variety of designs and changes to improve the evaporative surface area of solar distillers were developed in the hopes

* Corresponding author at: Department of Mechanical Engineering, College of Engineering in Al-Kharj, Prince Sattam bin Abdulaziz University, Al-Kharj, 11942, Saudi Arabia.
E-mail address: a.abdullah@psau.edu.sa (A.S. Abdullah).

https://doi.org/10.1016/j.est.2022.105647
Received 11 June 2022; Received in revised form 31 August 2022; Accepted 6 September 2022
2352-152X/© 2022 Elsevier Ltd. All rights reserved.

Fig. 1. Photographs of the investigated solar stills: (a) conventional drum solar still (DSS), (b) conventional drum, (c) corrugated drum solar still (CDSS), and (d) corrugated drum.

of increasing the distiller output [60]. Solar distillers with moving parts were offered as means of achieving that goal. The moving parts cause the molecules of water on the surface to break their bonds (surface tension) [7].

By putting a revolving fan inside the solar still, Kabeel et al. [37] enhanced the solar still productivity by 25 %. A rotating shaft was also installed within the distiller to increase its production [36]. In July, June, and May, the thermal efficiency was increased by 5.5 %, 5 %, and 2.5 %, respectively. Omara et al. [38] also put a revolving fan inside the conventional distiller and investigated its performance at different heights of saline water. They stated that at low speeds of fan, the basin water height should be as small as feasible. The freshwater production of a solar still combined with a revolving fan was increased by 17 %.

Covering the revolving parts with wick materials is an important modification to improve the daily production of the solar stills. For instance, Gad et al. [61] and Haddad et al. [62] proposed using horizontal and vertical rotating wick belts inside the conventional sill. Their technologies enhanced the surface areas of evaporation of the distiller without increasing the horizontal area. Additionally, Refs. [50,51] used a vertical and horizontal wick belt inside the conventional distiller in an attempt to utilize inside space for increasing the exposure surface and evaporative areas without the addition of more projected area to the

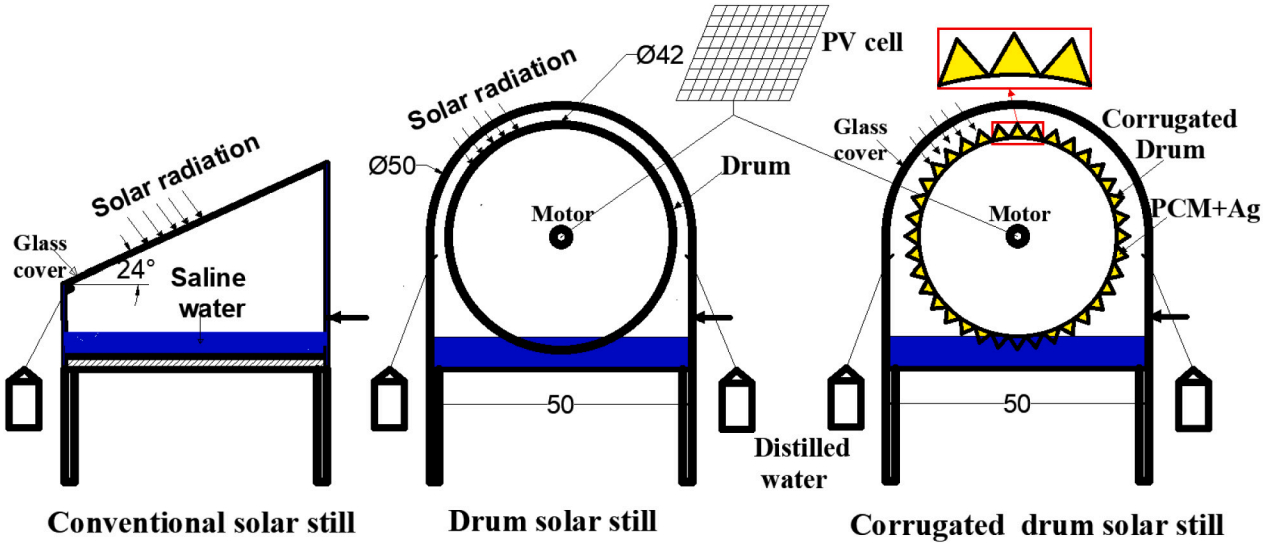

Fig. 2. Schematic diagram of the experimental setup with all investigated solar stills and PV panels.

solar still. They studied the still productivity and efficiency under various times of stop, and they concluded that the wick belt's optimal OFF time was 30 min with 5 min as ON time. They obtained an improvement of 315 % in solar still production.

The revolving cylinder is one of the spinning mechanisms used to increase the performance of solar stills. Ayoub et al. [63] investigated the effects of various parameters on the drum solar still performance, including speed of drum, basin water depth, and cover cooling. They came to the conclusion that the drum speed should be kept as low as possible without causing dry areas on the drum's surface. Also, Malaeb et al. [64] proposed a rotating cylinder within the solar distiller to improve the surface area of evaporative and reduce the thickness of saline water. This adjustment increased the solar still's freshwater productivity by 250 %. In addition, Essa et al. [46] published an experimental and empirical study for using a rotating drum with two different ends to increase the performance of a tubular distiller (opened and closed ends). With open ends drum and wick, they increased tubular distiller productivity by 175 % at 0.05 rpm. To increase the evaporation surface area, Abdullah et al. [65] included a rotating drum within the solar still. They evaluated the drum solar still's performance under a variety of operating settings of employing a condenser, solar air heater, nanofluid, and varying speeds of drum. They claimed that the conventional and drum distillers produced 2025 and 6420 mL/m^2.day, respectively. As a result of using the revolving drum, they enhanced productivity by 217 %.

The phase change materials (PCMs) are used for latent heat energy storage. They have the absorbing and releasing characteristics of thermal energy without temperature change under controlled conditions [66]. The PCM main advantages are the excellent storage capacity with small temperature variations and negligible volume changes, noncorrosive characteristics, congruent melting and so on [67]. While the main disadvantages of PCM are the low thermal conductivity, high volume variation, and seepage of liquid during state change [68]. PCM can be utilized to decrease the losses of heat during the peak sun irradiation, these materials can store energy and release it during the night when the irradiation is not available. In the absence of solar radiation, the PCM is the heat source for the water evaporation in the basin. Therefore, PCMs are able to improve the freshwater production of solar stills [69,70]. The rate of improvement in the case of adding nanoparticles to PCMs is dependent on the specific types of nanoparticles, PCMs, and system design [68].

Moreover, mixing paraffin wax with nanoparticles indicated superior performance as a PCM (Katekar et al. [71]). The influence of utilizing different nanoparticles materials (TiO_2, Al_2O_3 and CuO) on the performance of solar distiller was estimated by Sahota and Tiwari [72]. Using Al_2O_3 gave solar still exergy and thermal efficiency of 14.10 % and 50.34 %, respectively. Abdullah et al. [73] studied the effect of painting the surfaces of tubular distiller with the copper oxide nanoparticles and black paint mixture for the objective of improving the convective heat transfer coefficient between the basin surfaces and saline water. Results showed that the daily production was enhanced by 108 % over the conventional solar still by utilizing internal reflectors, nano coating and PCM with nanoparticles. Where, PCM can be utilized to decrease the heat losses. For example, during the maximum solar irradiation periods, PCM stores the energy of sun and releases this stored energy when the solar irradiation is not available at nighttime. An experimental study conducted by Alqsair et al. [74] to improve the performance of drum still utilizing transparent walls of solar still, nanoparticles' coating, PCM, parabolic solar concentrator (PSC), and external condenser. PSC was used to focus the sun rays on the drum's back side, which augmented the vaporization rate. It was concluded that the maximum productivity improvement was obtained for drum still with nano-coating, PSC and condenser, where the productivity was enhanced by 320 %.

Therefore, adding a revolving drum inside the solar still has some benefits, such as forming a thin water coating on the drum surface that quickly evaporates. The rotating drum also features a huge exposure surface and evaporative areas, which speed up the evaporation inside the distiller. Furthermore, due to turbulence in the water and water vapor contents inside the distiller, revolving the drum breaks the basin water surface tension.

Based on the deep literature conducted above, the effect of using corrugated drum on the performance of drum solar still is not investigated yet. So, the basic idea of this work is to improve the surface area of exposure to solar radiation and maximize the evaporative surface area of the drum by using corrugated drum. Also, using a corrugated drum surface increased the evaporative surface area of the drum solar still by 48 %. Consequently, the novel points of this work are as following.

1. The drum solar still integrated with a conventional and corrugated drum is investigated.
2. The influence of painting the corrugated drum by traditional black paint mixed with Ag-nanoparticles (nano-coating) was contemplated.
3. The corrugated drum solar still was studied under different speeds of rotational drum (0.05, 0.1, 0.3, 0.5, and 0.7 rpm).

Table 1
The design parameters and their values for all three solar stills.

No	Components	CSS	DSS	CDSS
1	Glass cover, 3 mm thick	Plan glass (0.62 m, L = 1 m)	Semi-circular glass (=0.5 m, L = 1 m)	
2	Basin dimensions	0.5 m × 1 m	0.5 m × 1 m	
3	Basin material, 1.5 mm thick	Galvanized steel sheet	Galvanized steel sheet	
4	Higher and lower walls	0.39 m and 0.16 m	0.25 m and 0.25 m	
5	Projected area	0.5 m^2	0.5 m^2	
6	Drum diameter and length	–	0.44 m and 0.98 m	
7	Drum material	–	Aluminum sheet 0.5 mm thick	
8	Drum surface	–	Smooth flat	Corrugated surface
9	Motor	–	Plate data (BBQ motor, Model No: MB-1, 12 V, 3WIPX4, Fuse rating: 630 mA)	

4. Adding a PCM mixed with Silver (Ag) nanoparticles to let the system operate during cloudy or sun absence was tested.
5. Environmental and economic analyses were carried out to make sure the reliability of the performance of the tested system.

2. Materials and procedures

2.1. Experimentation

Three solar stills (corrugated drum still (CDSS), conventional drum still (DSS), conventional still (CSS)), PV system, and DC electric motors were used in the experimental tests as illustrated in Figs. 1 and 2. For all measurements and productivity enhancement percentages of the other solar stills, the CSS was used as a reference still for performance comparison. The three studied distillers had the same projected area of 0.5 m^2. The CSS was made of a galvanized steel sheet with 1.5 mm thickness. To optimize the absorption of solar energy, the solar stills' surfaces were painted with matt black paint. Moreover, the heights of higher and lower walls of CSS were 0.39 m and 0.16 m, respectively. The CSS was covered by a glass sheet with 3 mm thick. The condensed droplets of freshwater were collected in a trough from the solar still and deposited into calibrated flasks. Furthermore, the basin was well-insulated with 50 mm thickness glass wool to avoid the loss of heat. A feeding water tank (Height = 1 m and diameter = 0.5 m) was utilized to feed the saline water to solar stills. The design parameters and their values for all three solar stills are obtained in Table 1.

On the other hand, a closed-ends drum was present in both the drum still (DSS) and the modified corrugated drum still (CDSS). As seen in Figs. 1 and 2, this drum was mounted on a shaft and rotated around its axis by a 3 watts DC electric motor. The revolving drum was built of 0.5 mm thick aluminum sheet (diameter = 0.44 m and length = 0.98 m). The motors were powered by a 10-watt photovoltaic system. The solar panel and battery made up the PV system. The electric motor was combined with a speed-controller to ensure that the drum rotated at the desired speed of rotational. To enhance the absorption of solar irradiation, the drum and solar stills were painted with a professional matt-black color. As indicated in Fig. 1 and Fig. 2, a semi-circular glass (diameter = 0.5 m and length = 1 m) was utilized to cover the DSS and CDSS. In addition, to get the distilled freshwater out of the drum still and into the freshwater bottles, it was collected into four troughs. For the solar still, a 30 mm thickness wooden box was utilized as a container. Also, silicone rubber was used as a sealing material to avoid the vapor leakage.

The corrugated drum still is the same as DSS except that the drum has a corrugated form with a vee length of 20 mm. The bending angle between any two bottoms or two tops is fabricated as 90°. So, the corrugated drum has 54 tops and 54 bottoms of corrugated form. The CDSS performance has been tested with paraffin wax mixed with Ag (Silver) nanoparticles, at 2.5 % mass fraction (975 g paraffin wax +25 g Ag), placed beneath the corrugated drum absorber as shown in Fig. 2. The fabrication of CDSS was assembled by revolving an aluminum cylinder, then 54 V-angles were welded on the outer surface of the cylinder. The V-shape (corrugated shape surface) had a vee width of 20 mm. Then, one end of the cylinder and all vees of this end were closed, and this part of cylinder was put into a boiling water to prevent the solidification of PCM during its filling. After that, the PCM was melted and put into the spaces of vees (Fig. 2), then the tops of vees were closed by welding.

Table 2
Thermo-physical properties of paraffin wax with and without Ag-nanoparticles.

Property	Paraffin wax with Ag-nanoparticles	Paraffin wax
Density	962 kg/m^3	876 kg/m^3
Melting point	53 °C	54.5 °C
Latent heat of fusion	182 kJ/kg °C	190 kJ/kg °C
Specific heat	2.01 kJ/kg °C	2.1 kJ/kg °C
Thermal conductivity	0.3 W/m °C	0.21 W/m °C

2.2. Proceeding of experiments

The whole setup was oriented to the south in order to maximize incident sun energy and tested in the environmental conditions of Kafrelsheikh, Egypt. Several metrics were measured hourly from 08:00 to 21:00 to evaluate the performance of the tested stills. Air temperatures, solar irradiation, speed of air, temperatures of water and glass cover temperature, and distilled freshwater amount were hourly measured. The tests were run for 13 h through the daytime and part of night, and the freshwater was daily measured. Saline water was used to feed the distillers from the feeding reservoir. A steady water depth was maintained in the three solar stills. Inside the distillers, there was a 20-mm depth of saline water. A thin layer of water was produced on the drum's outer surface with the first movement at the intended speed. The influence of sun radiation incident on the drum surfaces easily dissipated this film. As a result, vapor was created and rose to the inner surface of the glass cover, where it condensed.

To compare the productivity and efficiency of all distillers, we first analyzed the performance of the CSS, DSS, and CDSS without any extra modifications. This prompted a comparison of the modified drum solar still's performance to that of the others. The impact of the paint utilized to paint the corrugated surface of drum and Ag-nano with black paint has been considered. The influence of rotational drum speed on DSS and CDSS performances was investigated in the second part of the experiments. The speeds examined were 0.05, 0.1, 0.3, 0.5, and 0.7 rpm. DSS and CDSS were also compared to CSS in terms of thermal performance. The caves beneath the corrugated absorbers were filled with PCM mixed with Ag nanoparticles in the third phase to improve CDSS performance even more. The used nanoparticles were bought from the market. Silver nanoparticles have a thermal conductivity 419 W/m.K. By combining Ag-nanoparticles (10–20 nm in size) with paraffin wax, the low heat conductivity of the wax was improved. As a result, Ag-nanoparticles are utilized with paraffin wax as an enhancer of thermal conductivity. Ag-Nanoparticles have been added to the paraffin wax at 2.5 % mass fraction (25 g Ag + 975 g wax). The properties of the wax and wax with 2.5 wt% nanoparticles are presented in Table 2. From previous research work [40], the authors found that increasing nanoparticles' concentration mixed with the paraffin wax increases the thermal conductivity of wax till reaching 2.5 wt%, after that the thermal conductivity become stable. This is why 2.5 wt% Ag concentration is taken in this study. The weight of the PCM-Ag is about 8 kg. The Differential Scanning Calorimetry (DSC) of paraffin wax with Ag-nanoparticles is presented in Fig. 3. It is worth to mention that the PCM is located at the bottom of the

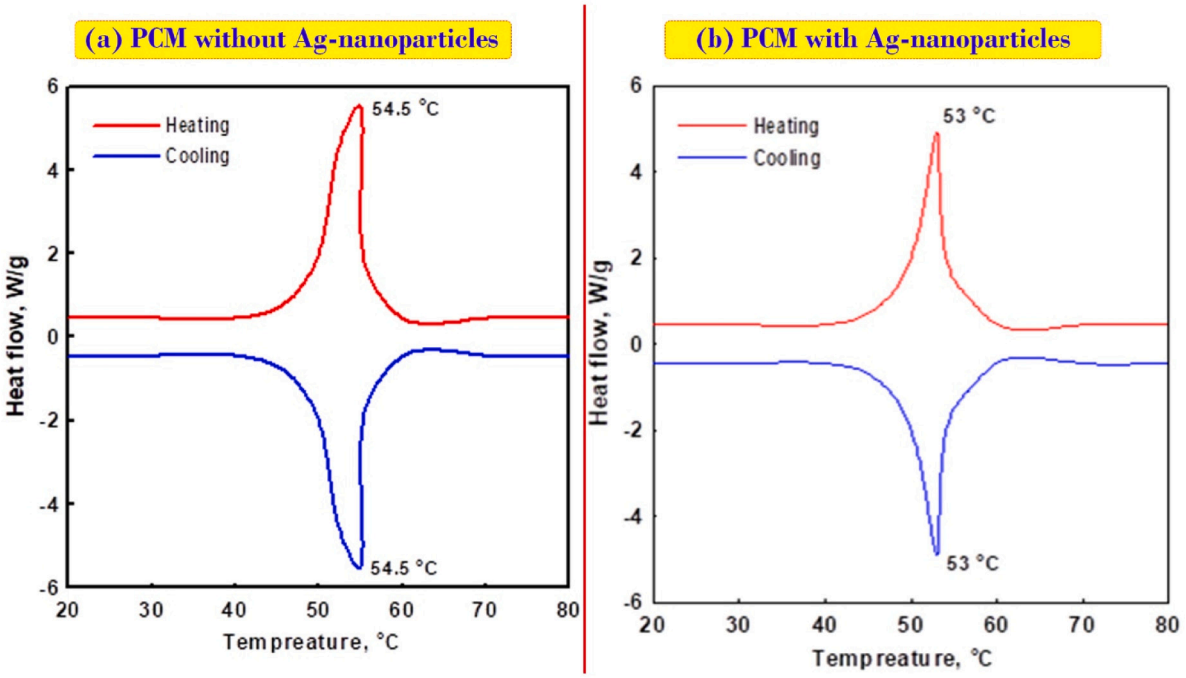

Fig. 3. Differential Scanning Calorimetry (DSC) curves of the paraffin wax (PCM) with and without Ag nanoparticles.

Table 3
The details of the measuring devices.

Device	Parameter	Unit	Resolution	Accuracy	Range	Error
Solar power meter	Solar radiance	W/m^2	0.1 W/m^2	±1 W/m^2	0–5000 W/m^2	1.6 %
K-type thermocouple	Temperature	°C	0.1 °C	±0.5 °C	0–100 °C	1.3 %
Anemometer	Air speed	m/s	0.01 m/s	±0.1 m/s	0.4–30 m/s	1.1 %
Graded bottles	Yield	L	0.01 L	±0.2 L	0–25 L	1.3 %

corrugated absorber, as shown in Fig. 2, where the PCM is located inside the triangle whose sides are 2 cm by 2 cm and its base is approximately 3 cm, so the thickness of the wax is different because it is a triangle shape.

2.3. Instruments for measuring

With the help of the appropriate instruments, the various parameters impacting the performance of solar stills were measured. The irradiation of sun was hourly monitored with a zero to 5000 W/m^2 solar power meter. Temperature was measured at several points across the system using calibrated K-type thermocouples. Furthermore, a G4L-CUEA MPLC (modular programmable logic control) was utilized to measure the thermocouple signal and acquire digital temperature measurements. An anemometer of the van type was used to monitor the air velocity. Furthermore, the calibrated graded bottles recorded the freshwater distillate hourly.

2.4. Uncertainty analysis

The analyses of uncertainty for all the experimental instruments were estimated using Ref. [75]. The result uncertainty is determined by:

$$W_R = \sqrt{\left(\frac{\partial R}{\partial X_1}W_1\right)^2 + \left(\frac{\partial R}{\partial X_2}W_2\right)^2 + \ldots + \left(\frac{\partial R}{\partial X_n}W_n\right)^2}$$

where W_1, W_2, W_3, ..., W_n are the uncertainties of independent factors. The errors in the measurements of the devices are tabulated in Table 3. Also, the yield is a function of water depth; m = f(h). Hence, the yield uncertainty is:

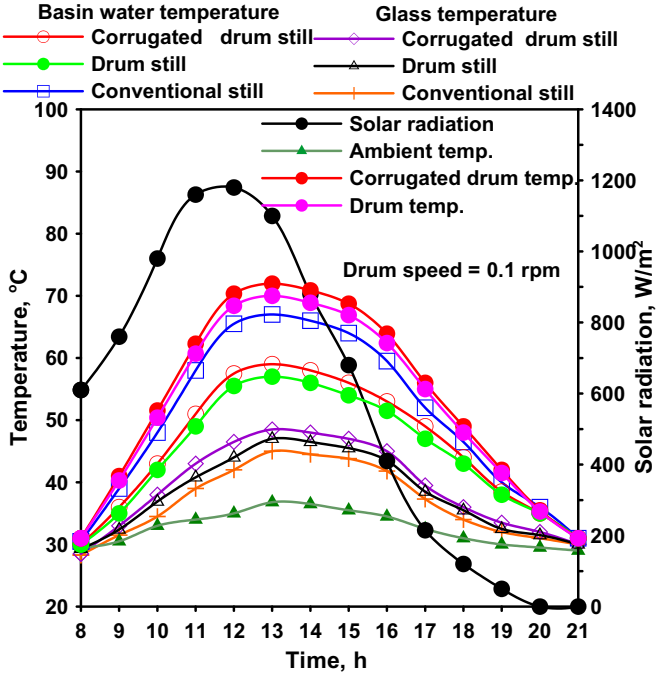

Fig. 4. Temperatures of glass, water and corrugated drum of solar stills and ambient conditions (solar radiation and ambient air temperature).

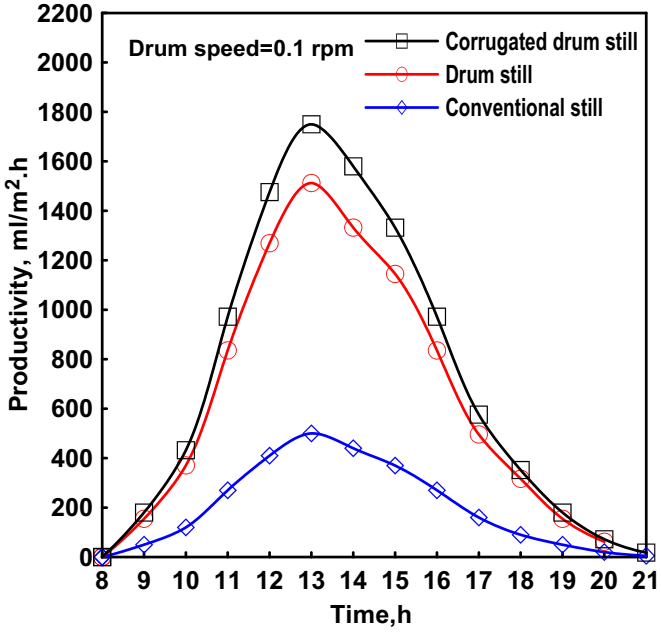

Fig. 5. The hourly productivity of the CSS, DSS, and CDSS at 0.1 rpm.

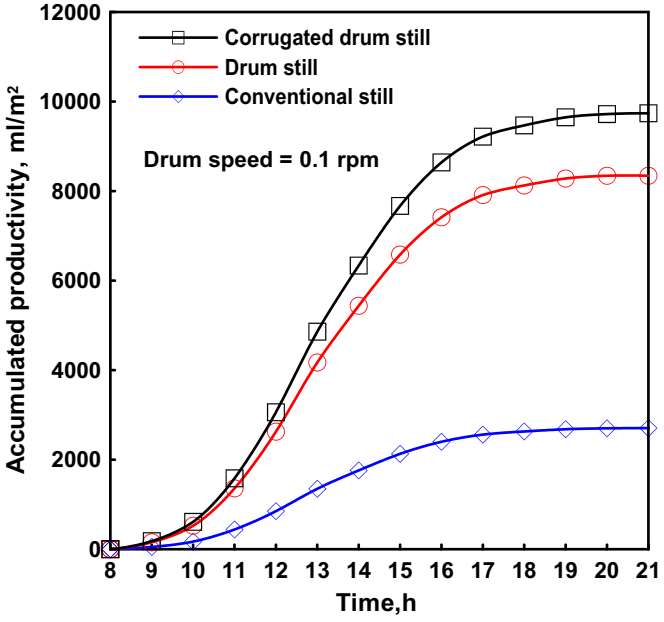

Fig. 6. The total accumulated productivity of the CSS, DSS, and CDSS at drum speed of 0.1 rpm.

$$W_m = \sqrt{\left(\frac{\partial m}{\partial h_1} W_h\right)^2}$$

Also, the uncertainty in efficiency (η) is:

$$W_{\eta_{th}} = \sqrt{\left(\frac{\partial \eta_{th}}{\partial m} W_m\right)^2 + \left(\frac{\partial \eta_{th}}{\partial I_R} W_{I(t)}\right)^2}$$

Consequently, the uncertainty of yield and efficiency of distillers are ±1.5 % and ±2.3 %, respectively.

3. Results and discussion

3.1. Rotating drum distillers' performance

Temperatures of basin water and glass cover of the solar distillers and corrugated absorber temperature at 0.1 rpm and the ambient conditions (air temperature and solar radiation) are shown in Fig. 4. The temperature of water in the DSS is found to be 0–10 °C lower than in the CSS. This happens because the water is warmed and heated by the drum's heat rather than directly by the incident sun energy. The water in the CSS is heated directly by the sun radiation. So, the DSS's water temperatures are lower than the CSS's. On the other hand, due to the high rate of evaporation within the DSS, the temperature of glass of the CSS is 0–2 °C lower than that of the DSS.

Furthermore, the CDSS's basin water temperature is lower than that of the CSS by 0–8 °C. In addition, the average temperature of the corrugated drum of the CDSS was higher than the water temperature of the CSS by 5 °C, Fig. 4. This result leads to a faster evaporation process inside the CDSS. Besides, the CDSS has a temperature of glass higher than that of CSS by 0–3.5 °C due to the high evaporation rate generated inside the CDSS. Furthermore, at 12:00, the maximum solar irradiation was recorded as 1180 W/m^2. At 13:00, the highest temperature of water was recorded, where the temperatures of water of CDSS, DSS, and CSS were 59, 57, and 67 °C, respectively, and the average temperature of the corrugated drum reached to 72 °C. While the glass temperatures were reported as 48.5, 47, and 45 °C for the CDSS, DSS, and CSS at 13:00, respectively.

Fig. 5 depicts the solar distillers' hourly productivity at 0.1 rpm drum speed. It was discovered that the production increases from 0.0 at the start of experiment to its highest value at noon, then declines again in the afternoon. At 13:00, the solar stills' hourly production was measured. Where, the maximum production of the CDSS, DSS, and CSS was 1750, 1500, and 500 mL/m^2, respectively. The hourly production of the DSS is higher than that of CSS as seen in Fig. 5. This is owing to the higher rate of evaporation caused by the thin water layer effect on the body of drum as compared to the CSS. The DSS has a larger surface area for evaporation than the CSS. Additionally, the DSS had a larger solar radiation exposure area, which increased vapor formation when compared to the CSS. The DSS has a 0.69 m^2 exposure area compared to merely 0.5 m^2 for CSS. As a result, when compared to the CSS, the DSS produces more evaporation. Additionally, the drum rotation creates turbulence in the saline water of basin, which causes the surface connections between water molecules to break. As a result, the evaporation and water production rise.

Fig. 5 shows that the hourly production of the CDSS is higher than that of either DSS or CSS. This is because the CDSS has a drum temperature higher than he drum temperature of DSS and the water temperature of CSS. The temperature of the corrugated drum was higher than the normal one by 0–1.5 °C (Fig. 4). Additionally, the surface area of evaporative the CDSS is greater than that of the other solar stills. When compared to the other distillers, this results in a higher vapor generation inside the CDSS. Additionally, the exposure area to solar irradiation for the CDSS is higher than that of the DSS and CSS due to utilizing the corrugated drum. Where, the exposure area of the CDSS equals 1 m^2 compared to 0.69 and 0.5 m^2 for DSS and CSS, respectively. So, the percentage of increase of the exposure area of the CDSS equals 45 % and 100 % over DSS and CSS, respectively. Additionally, the evaporated area of the CDSS equals 2 m^2 compared to 1.35 and 0.5 m^2 for DSS and CSS, respectively. So, the percentage of increase of the evaporated area of the CDSS equals 48 % and 330 % over DSS and CSS, respectively. In the event that the sides of the cylinder are taken into account, the evaporated area of the CDSS equals 2.3 m^2 compared to 1.65 and 0.5 m^2 for DSS and CSS, respectively. So, the percentage of increase of the evaporated area of the CDSS equals 40 % and 360 % over DSS and CSS, respectively.

The total accumulated production of the tested stills at 0.1 rpm is shown Fig. 6. The total production of DSS is higher than that of CSS. Furthermore, the CDSS has a greater total distillate than either the DSS

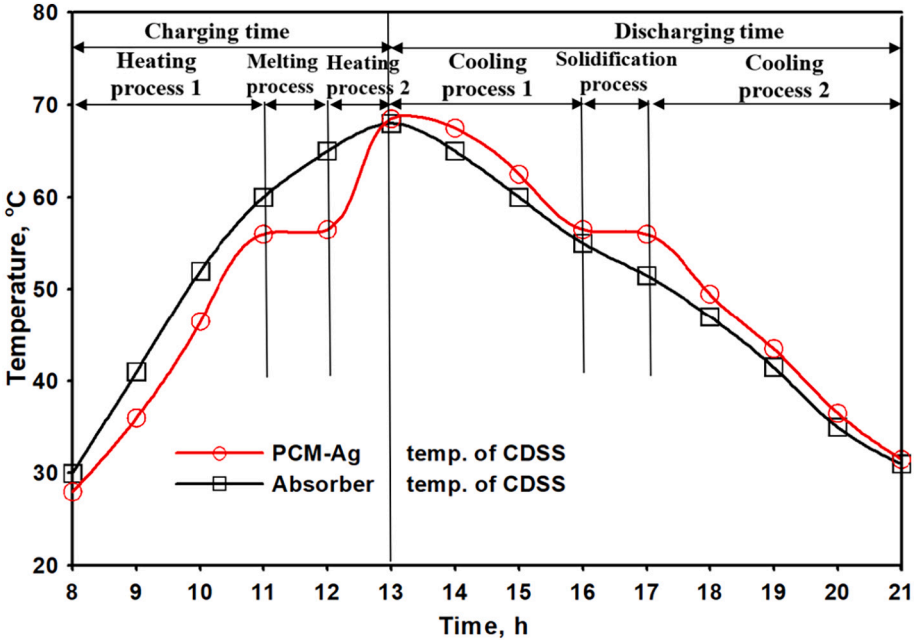

Fig. 7. Temperature variations of the corrugated drum absorber and PCM-Ag for CDSS.

or CSS. The accumulated production of the CDSS, DSS, and CSS are 9700, 8350, and 2700 mL/m^2. day, respectively. As a result, the yield generation is enhanced by 260 % and 209 % when utilizing the CDSS and DSS over the CSS, respectively. Where, the percentage of increase of the exposure area of the CDSS equals 45 % and 100 % more DSS and CSS, respectively. In addition, the percentage of increase of the evaporated area of the CDSS equals 48 % and 330 % over DSS and CSS, respectively.

3.2. *Effect of incorporating Ag nanoparticles into black paint*

The black paint has been mixed with 2.5 % silver nanoparticles, and the combination is utilized to paint the drum's corrugated surface. The goal of mixing Ag-Nano with black paint is to improve the corrugated surface's thermal conductivity and absorption rate. The effect of employing Ag-Nano in black paint on CDSS performance has been investigated and compared. The specific heat capacity, optical characteristics and thermal conductivity of the nanoparticles are all factors in their selection. When compared to CuO (76.5 W/mK) and TiO_2 (4.8 W/mK), silver has the maximum thermal conductivity (419 W/mK). Silver's excellent thermal conductivity resulted in a high-water temperature and rate of evaporation. The daily production of CDSS with Nano black paint was roughly 280 % higher than CSS, whereas it was 260 % without Ag-black paint, according to the experimental data. This means that combining Ag-black paint with CDSS resulted in a 20 % boost in daily output. The daily productivity of CDSS with Ag-black paint was 10,650 mL/m^2 per day, while CSS produced around 2800 mL/m^2 per day.

3.3. *Performance of CDSS when using PCM-Ag nanoparticles*

PCM can be utilized to decrease the losses of heat during the peak sun irradiation. The PCM materials can store energy and release it during the night when the solar irradiation is not available. In the absence of the solar radiation, the PCM is the heat source for the water evaporation in the basin. The paraffin wax was placed beneath the corrugated absorber of CDSS, to absorb the thermal energy from the wetted drum during the time of charging and releases it back to water through the corrugated absorber during time of discharge. When the temperature of the paraffin wax is within the melting point range, heat is stored as latent heat, and when it is outside this range, heat is stored as sensible heat as shown in Fig. 7. Ag-Nano improves thermal conductivity while lowering melting

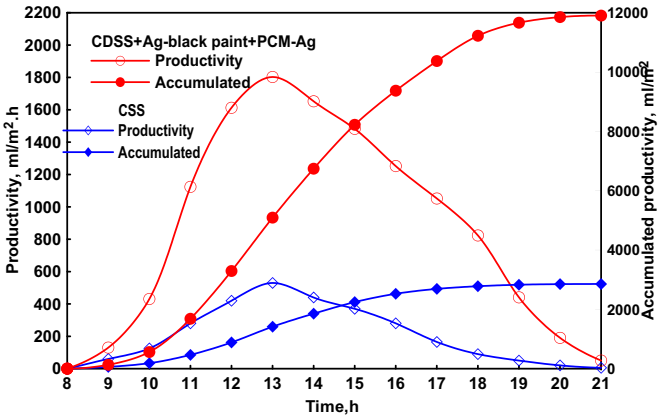

Fig. 8. Hourly and cumulative productivities for CSS and CDSS with PCM-Ag.

temperatures (54.5 °C without Ag and about 53 °C with Ag) and temperatures of solidification compared to paraffin wax without Ag-Nano. The improvement in thermal conductivity (0.21 W/m °C without Ag and about 0.3 W/m °C with Ag) helps in decreasing the time of charging of the paraffin wax during the period of melting, while the improvement in heat release rate accelerates solidification. Sari and Karaipekli [76] came at the same conclusion.

The influence of utilizing paraffin wax mixed with Ag-nanoparticles as thermal energy storage has been indicated in this part. Fig. 7 indicates the variations of corrugated drum and PCM-Ag temperature for CDSS with time. In the figure, the PCM and corrugated absorber temperatures have been incremented from the morning to the highest value at around 13:00. In the case of PCM-Ag, the temperature increase is different because it has constant temperatures time where the PCM-Ag transitions from a solid to a liquid state (process of melting) from about 11:00 to 12:00. The temperatures of paraffin wax rise gradually from 8:00 to 11:00 (process of heating 1) and from 12:00 to 13:00 (process of heating 2).

After 13:00, the sun irradiation began to decline, and the temperatures of the absorber and paraffin wax began to decay as shown in Fig. 7. After 13:00, heat is transferred from wax to the absorber and water. At

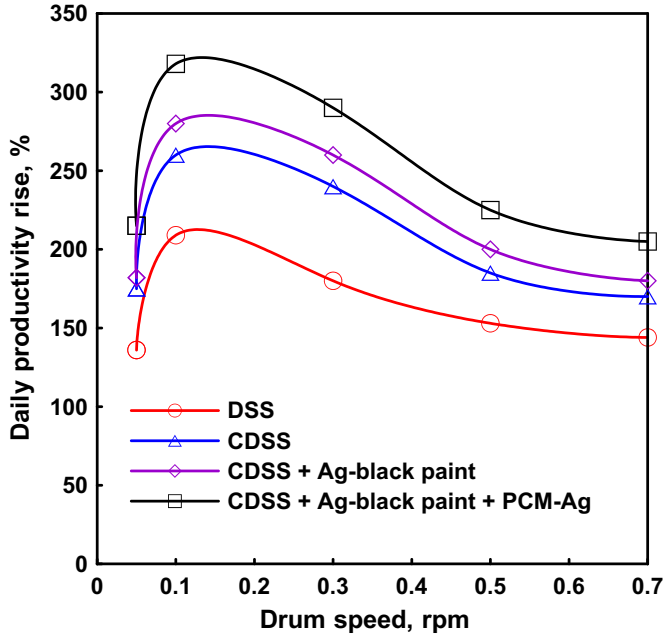

Fig. 9. Enhancement of productivity for the CDSS at different drum speeds under various operating conditions compared to the productivity of DSS.

16:00, the wax began to harden, and by 17:00, it was entirely solid (process of solidification). As illustrated in Fig. 7, the temperature of the paraffin wax was reduced from 13:00 to 16:00 (process of cooling 1), and then from 17:00 to 21:00 (process of cooling 2), until it reached the ambient temperature. Furthermore, the figure depicted that the temperatures differential between the drum surface and the water is not significant throughout the process of charging. However, due to the heat transferred from the paraffin wax to the corrugated absorber during the discharging process, this discrepancy is greater.

The productivity of CSS and CDSS with PCM-Ag and Ag-black paint has been compared and shown in Fig. 8. Fig. 8 indicates that, from 8:00 to 10:00, the production for CDSS and CSS is not very different. After 10:00, the disparity between the tested still's production grew steadily over time, peaking about 13:00. In addition, Fig. 8 indicated that the yield for CDSS and CSS are 11,900 and 2850 mL/m^2 day, respectively. So, the CDSS with PCM-Ag and Ag-black paint indicated about 318 % higher production than CSS. In addition, it can be said that utilizing PCM-Ag improved the production of CDSS by around 38 %, because the improvement in CDSS production was 280 % when utilizing Ag-black paint only. The use of paraffin wax-CuO nanoparticles (2.5 %) in a previous author's research [77] increased the productivity of a solar still with corrugated wick by roughly 32 %. But, in the present study, the improvement in production is 38 %, this is owing to Ag-superior nano's thermophysical characteristics over CuO-nano.

3.4. The influence of speed of drum on DSS performance

In this part, we investigated the impact of varying drum speeds on DSS performance in various operational scenarios. Fig. 9 shows the daily production rise of the DSS as compared to the CSS at various rotating cylinder (drum) speeds. For the DSS without any modifications, the water production was enhanced with increasing the speed of drum till the optimum speed at 0.1 rpm, where the production rise was improved by about 209 % over the CSS. The percentage of DSS productivity improvement was then reduced by raising the drum speed to only 144 % at 0.7 rpm. This is owing to the rotating drum's high speeds reduces the evaporation rate. Furthermore, when compared to the CSS, the DSS improved the output by 136 % at 0.05 rpm. As a result of the slow speed, dry spots appear on the drum, accounting for low percentage of productivity improvement.

For the case of integrating DSS with corrugated drum (first modification), the CDSS productivity rise at all drum speeds is indicated in Fig. 9. Also, the water production of the CDSS was enhanced with increasing the drum speed till the optimum speed at 0.1 rpm, where the production rise was reached about 260 % over the CSS. At 0.05 rpm, the productivity increase was only about 39 % (136 % for DSS with conventional drum versus 175 % with corrugated drum). This is because some dry bits forming on the corrugated drum due to the low speed.

In the second modification, mixing Ag-nano with the black paint resulted in an increase in CDSS production at all drum speeds. The productivity rise of CDSS with Ag-black paint was minimal at low speed also, with a productivity improvement of just 7 % at 0.05 rpm (175%for CDSS without versus 182 % with Ag-black paint). At 0.1 rpm, the CDSS's greatest productivity increase was 280 %. The productivity rise of the CDSS with Ag-black paint was then reduced when the drum speed was increased more than 0.1 rpm. In the final case, the productivity increase of CDSS with Ag-black paint and PCM-Ag was limited at low speeds, with only 30 % productivity improvement at 0.05 rpm (182 % for CDSS without PCM-Ag versus 211 % with PCM-Ag). Furthermore, employing the PCM boosted the productivity as the drum speed was raised. At 0.1 rpm, the CDSS increased its productivity by 318 % with PCM-Ag.

From this work, it is clear that the best speed of rotation of the cylinder is 0.1 rpm, and this is consistent with many publications as in Table 4. We note from the table that in the case of a wick enveloped the cylinder, we need a small speed of 0.5 rpm because it takes time for evaporation. In solar terms, the optimum speed became 0.3 rpm because the evaporation rate was fast, so this increased the speed of the cylinder because at the speed of 0.1 rpm, drying occurs on some parts of the cylinder.

The formula used to compute the daily thermal efficiency, (η_d), for the examined distillers is as follows [37];

$$\eta_d = \frac{\sum \dot{m} \times h_{fg}}{\sum A \times I(t) + MP}$$

where h_{fg}, $\dot{m}$, A, $I(t)$, and MP are vaporization latent heat, hourly

Table 4
Comparison between this work and others in the point of rotational speed and productivity rise.

No	Author	Solar still type	Drum type	Additions	Optimum speed, rpm	Productivity rise, %
1	Malaeb et al. [64]	Drum solar still	Smooth	–	0.1	250
2	Abdullah et al. [65]	Drum solar still	Smooth	–	0.1	217
3	Essa et al. [46]	Tubular solar still	Smooth	–	0.1	135
				Wick	0.05	175
4	Essa et al. [78]	Tubular solar still	Smooth	–	0.1	135
				Parabolic solar concentrator (PSC)	0.3	195
5	Abdullah et al. [53]	Conventional SS	Smooth	–	0.1	266
				Wick	0.05	280
6	Alqsair et al. [74]	Transparent CSS	Smooth	–	0.1	203
				PSC + external condenser	0.3	320
7	Present study	Drum solar still	Corrugated	–	0.1	260
				PCM-Ag	0.1	318

Table 5
Tested solar stills efficiency at different drum speeds under different conditions.

rpm	CSS	DSS	CDSS	CDSS + Ag-black paint	CDSS + Ag-black paint + PCM-Ag
0.05	33.5	52.5	58.2	59.3	63.2
0.1	34	63.3	71	74	79
0.3	33.8	59	68	71	75.5
0.5	33.3	55	59.5	62	65.7
0.7	33.5	52.1	57.4	59	62.6

Table 6
Fixed costs of fabricated CSS and modified CDSS for 1 m^2.

Unit	Cost of CSS ($)	Cost of modified CDSS ($)
Aluminum drum	–	20
Glass cover	10	15
Iron sheet	30	10
Paint	10	5
Support legs and ducts	25	25
Production	20	65
Fiberglass	7	7
DC-Motor (3 W)	–	10
Photovoltaic system	–	50
Nanoparticles	–	30
PCM	–	13
Total fixed cost (F)	102	250

distillate productivity, system area (projected area of distiller + projected area of PV), daily average solar radiation, and motor power.

Table 5 shows the daily thermal efficiency of the tested distillers at varying drum speeds, based on the given relationship. So, Table 5 shows the variations in the DSS's average daily thermal efficiency under various operating situations based on the aforesaid relationships. Table 5 shows that the lowest and highest DSS efficiencies without any modification were found at 0.07 and 0.1 rpm, respectively, with efficiency of 52.1 % and 63.3 %, respectively. The thermal efficiency of the CDSS at 0.05 rpm was 58.2 % (instead of 52.5 % without using corrugated drum). Additionally, the CDSS's maximum efficiency was achieved at 0.1 rpm, where it was about 71 % as a result of the increased output at this speed. From Table 5, at all rotating speeds, utilizing the Ag-black paint increased the thermal efficiency of the CDSS. Where, the CDSS's highest efficiency was 74 % at 0.1 rpm with an improve in thermal efficiency by 3 % over that of the CDSS without Ag-black paint. Also, at all rotating speeds, utilizing the PCM-Ag increased the efficiency of the CDSS. The DSS's highest efficiency with PCM-Ag was 79 % at 0.1 rpm with an improve in efficiency by 5 % over that of the CDSS without PCM-Ag. Furthermore, the CSS's efficiency was about 33–34 %.

3.5. Cost analysis of tested solar stills

The cost of distillers (Table 6) is determined by the type of distiller and its separate components. So, the estimated cost is conducted for both variable cost and fixed cost. Based on the average daily freshwater production and the lifetime of solar still, the total cost of 1 L from the distiller can be obtained as follows:

The total fixed cost (F) of conventional SS = 102 $/L.$m^2$. The total cost per year C is assumed as;

$$\textit{The annual total cost}\ (C) = \textit{fixed cost}\ (F) + \textit{variable cost}\ (V)$$

According to [79,80], let variable cost equals 0.3 fixed cost per year. It also includes the expense of upkeep. Let the expected lifetime of solar still is about 10 years, then The annual total cost (C) = 102 + (102 × 0.3 × 10) = 408 $. The still operates around 340 days in a year and the average freshwater production is about at 2.5 L/m^2.day. The freshwater yield during the life of CSS is 340 × 2.5 × 10 = 8500 L. The potable water cost of 1 L from a CSS =408/8500 = 0.048 $.

The total fixed cost of CDSS (with Ag-black paint and PCM-Ag) per 1 m^2 is about 250 $. Then, C = 250 + (250 × 0.3 × 10) = 1000 $. The average freshwater production is about 7.6 L/m^2 day. The freshwater yield of CDSS is 7.6 × 340 × 10 = 25840 L. The potable water cost of l L from CDSS = 1000/25840 = 0.039 $.

So, the potable water cost of 1 L from the CSS and CDSS equals to 0.048 $ and 0.039 $, respectively.

Table 7
Components embodied energy.

Components	Material	Energy density, kW.h/kg	Mass, (kg)	Embodied energy, E_{in} (kW.h)
Drum	Aluminum	8.8	10	176
basin	Steel	13.8	10	138
Cover and walls	Glass	4.16	9	37.4
Valves	Brass	17.22	0.22	3.8
Coating	Black paint	25	0.2	5
Total				360

3.6. Environmental analyses

In this part, the proposed system's environmental analyses are assessed. It is well knowledge that the world has recently been paying great attention to environmental analyses of systems in order to learn about greenhouse gas emissions, particularly CO_2, and evaluation of the life cycle (Mehrpooya and Mousavi [81]).

This sparked curiosity because the usage of fossil fuels causes calamities and environmental dangers such as the release of greenhouse gases into the atmosphere. This aided scientists and decision-makers in deciding to use renewable energy sources for systems rather than fossil fuels in order to fulfill sustainability and environmental preservation goals. The following are the suggested governing equations for CO_2 emission and mitigation by solar still (yearly and over the lifespan of the system):

The solar still annual energy output (kW.h/year) is

$$E_{out} = \frac{365 \times \dot{m}(\text{hourly yield}) \times h_{fg}(\text{latent heat of vaporization})}{3600}$$

In kilograms per year, the quantity of CO_2 emitted (Parsa et al. [82]).

$$CO_{2,emitted} = \frac{2 \times E_{in}}{n}$$

where, E_{in} is the components embodied energy.

The amount of CO_2 emitted over the system's lifespan is then calculated:

$$CO_{2,emitted} = 2 \times E_{in}$$

Furthermore, the amount of CO_2 reduced in kg/year during the course of the year is:

$$CO_{2,mitigated} = \frac{2 \times E_{out}}{n}$$

In addition, the amount of CO_2 mitigated in kg during the system lifespan is:

$$CO_{2,mitigated} = 2 \times E_{out} \times n$$

The environmental parameters (ϕ_{CO_2} and Z') are obtained as following:

$$\phi_{CO_2} = \frac{2 \times ((E_{out} \times n) - E_{in})}{1000}$$

And,

$$Z' = z_{CO_2} \times \phi_{CO_2}$$

where, z_{CO_2} is the cost of carbon (Parsa et al. [82]) in the international

Table 8
Enviroeconomic and environmental analysis for lifetime 20 years and 365 days.

CDSS with modifications	Embodied energy = E_{in} (kW.h))	E_{out} yearly (kW.h)	E_{out} for lifetime (kW.h)	Enviroeconomic parameter, (Z'. year)	Environmental parameter, (ϕ_{CO_2}. year)
	360	370	7400	200.4	14

market (14.5 $/ton).

Regarding the above equations, the embodied energy of the system components is tabulated in Table 7. Additionally, the enviroeconomic and environmental analyses for lifetime 20 years and 365 days are obtained in Table 8. So, the environmental parameter of CDSS with modifications (with Ag-black paint and PCM-Ag) was 14 tons CO_2 per year. Also, the enviroeconomic parameter (Z') was 200.4 per year for the CDSS with modifications (with Ag-black paint and PCM-Ag), for lifetime 20 years and 365 operating days, Table 8.

4. Conclusions

The current study examines the performance of a drum solar still with certain changes in an experimental setting. The modifications included using a corrugated drum of DSS, Ag-nanoparticles' coating and PCM-Ag. DSS's performance was also put to the test at various rotating speeds of drum. The following points have been addressed:

1. At 0.1 rpm, the highest increase in productivity for both DSS and CDSS was reached. The daily production was enhanced by 209 % and 260 % when utilizing the DSS and CDSS over that of CSS, respectively. Where, the evaporated area of the CDSS equals 2.3 m^2 compared to 1.65 and 0.5 m^2 for DSS and CSS, respectively.
2. Using the Ag-black paint improved the performance of CDSS, where the total yield increased by 280 % over the CSS at 0.1 rpm with thermal efficiency 74 %.
3. The CDSS with Ag-black paint and PCM-Ag improved the productivity by 318 % over the CSS at 0.1 rpm, with thermal efficiency of 79 %.
4. The modified CDSS is capable to mitigate 14 tons of CO_2 per year. Where, the solar energy is not needing the burning process that other fuels need, but rather gives its users clean and pure energy that is not negatively affect the surrounding environment and its elements.
5. The desalinated freshwater costs were found to be 0.048 and 0.039 $/L for the CSS and for modified CDSS, respectively.

Declaration of competing interest

The authors declare that they have no known competing financial interests or personal relationships that could have appeared to influence the work reported in this paper.

Data availability

No data was used for the research described in the article.

Acknowledgments

The authors extend their appreciation to the Deputyship for Research & Innovation, Ministry of Education in Saudi Arabia for funding this research work through the project number (IF-PSAU-2021/01/17978).

References

[1] Z. Omara, A. Kabeel, The performance of different sand beds solar stills, Int. J. Green Energy 11 (3) (2014) 240–254.
[2] M. Younes, A. Abdullah, F. Essa, Z. Omara, Half barrel and corrugated wick solar stills–comprehensive study, J. Energy Storage 42 (2021), 103117.
[3] Z.M. Omara, M.A. Eltawil, Hybrid of solar dish concentrator, new boiler and simple solar collector for brackish water desalination, Desalination 326 (2013) 62–68.
[4] M.A. Eltawil, Z. Omara, Enhancing the solar still performance using solar photovoltaic, flat plate collector and hot air, Desalination 349 (2014) 1–9.
[5] A.R. Abd Elbar, H. Hassan, Enhancement of hybrid solar desalination system composed of solar panel and solar still by using porous material and saline water preheating, Sol. Energy 204 (2020) 382–394.
[6] A.E. Kabeel, A. Khalil, Z.M. Omara, M.M. Younes, Theoretical and experimental parametric study of modified stepped solar still, Desalination 289 (2012) 12–20.
[7] M.R. Diab, F.A. Essa, F.S. Abou-Taleb, Z.M. Omara, Solar still with rotating parts: a review, Environ. Sci. Pollut. Res. 28 (39) (2021) 54260–54281.
[8] Z.M. Omara, A.E. Kabeel, M.M. Younes, Enhancing the stepped solar still performance using internal reflectors, Desalination 314 (2013) 67–72.
[9] K.M. Bataineh, M.A. Abbas, Performance analysis of solar still integrated with internal reflectors and fins, Sol. Energy 205 (2020) 22–36.
[10] Z. Cui, L. Kang, L. Li, L. Wang, K. Wang, A combined state-of-charge estimation method for lithium-ion battery using an improved BGRU network and UKF, Energy 259 (2022), 124933.
[11] D. Li, L. Wang, C. Duan, Q. Li, K. Wang, Temperature prediction of lithium-ion batteries based on electrochemical impedance spectrum: a review, Int. J. Energy Res. 46 (8) (2022) 10372–10388.
[12] C. Liu, D. Li, L. Wang, L. Li, K. Wang, K. L, D.H. L, D. J, J.X. R, Z. S, Z.Y. J, Strong robustness and high accuracy in predicting remaining useful life of supercapacitors synthesis and catalytic performance of a new V-doped CeO2-supported alkali-activated-steel-slag-based photocatalyst, APL Mater. 10 (6) (2022), 061106.
[13] Q. Li, D. Li, K. Zhao, L. Wang, K. Wang, State of health estimation of lithium-ion battery based on improved ant lion optimization and support vector regression, J. Energy Storage 50 (2022), 104215.
[14] F.A. Essa, M. Abd Elaziz, A.H. Elsheikh, An enhanced productivity prediction model of active solar still using artificial neural network and Harris hawks optimizer, Appl. Therm. Eng. 170 (2020), 115020.
[15] F.A. Essa, M. Abd Elaziz, A.H. Elsheikh, Prediction of power consumption and water productivity of seawater greenhouse system using random vector functional link network integrated with artificial ecosystem-based optimization, Process Saf. Environ. Prot. 144 (2020) 322–329.
[16] M. Abd Elaziz, F.A. Essa, A.H. Elsheikh, Utilization of ensemble random vector functional link network for freshwater prediction of active solar stills with nanoparticles, Sustainable Energy Technol. Assess. 47 (2021), 101405.
[17] S. Pavithra, T. Veeramani, S.S. Subha, P.S. Kumar, S. Shanmugan, A.H. Elsheikh, F. Essa, Revealing prediction of perched cum off-centered wick solar still performance using network based on optimizer algorithm, Process Saf. Environ. Prot. 161 (2022) 188–200.
[18] Y.A.F. El-Samadony, A.S. Abdullah, Z.M. Omara, Experimental study of stepped solar still integrated with reflectors and external condenser, Exp. Heat Transfer 28 (4) (2015) 392–404.
[19] H. Amiri, M. Aminy, M. Lotfi, B. Jafarbeglo, Energy and exergy analysis of a new solar still composed of parabolic trough collector with built-in solar still, Renew. Energy 163 (2021) 465–479.
[20] O. Bait, Exergy, environ–economic and economic analyses of a tubular solar water heater assisted solar still, J. Clean. Prod. 212 (2019) 630–646.
[21] W.H. Alawee, F.A. Essa, S.A. Mohammed, H.A. Dhahad, A.S. Abdullah, Z. M. Omara, Y. Gamiel, Improving the performance of pyramid solar distiller using dangled cords of various wick materials: novel working mechanism of wick, Case Stud. Therm. Eng. 28 (2021), 101550.
[22] W.M. Farouk, A.S. Abdullah, S.A. Mohammed, W.H. Alawee, Z.M. Omara, F. A. Essa, Modeling and optimization of working conditions of pyramid solar still with different nanoparticles using response surface methodology, Case Stud. Therm. Eng. 33 (2022), 101984.
[23] W.H. Alawee, A. Abdullah, S.A. Mohammed, H.A. Dhahad, Z. Omara, F. Essa, Augmenting the distillate yield of cords pyramid distiller with baffles within compartments, J. Clean. Prod. 356 (2022), 131761.
[24] M.E.H. Attia, A.E. Kabeel, M. Abdelgaied, F.A. Essa, Z.M. Omara, Enhancement of hemispherical solar still productivity using iron, zinc and copper trays, Sol. Energy 216 (2021) 295–302.
[25] Z.M. Omara, A.E. Kabeel, A.S. Abdullah, F.A. Essa, Experimental investigation of corrugated absorber solar still with wick and reflectors, Desalination 381 (2016) 111–116.
[26] Z.M. Omara, A.E. Kabeel, F.A. Essa, Effect of using nanofluids and providing vacuum on the yield of corrugated wick solar still, Energy Convers. Manag. 103 (2015) 965–972.
[27] Z. Omara, M.H. Hamed, A. Kabeel, Performance of finned and corrugated absorbers solar stills under Egyptian conditions, Desalination 277 (1–3) (2011) 281–287.
[28] Z. Omara, M.A. Eltawil, E.A. ElNashar, A new hybrid desalination system using wicks/solar still and evacuated solar water heater, Desalination 325 (2013) 56–64.
[29] V.K. Ramalingam, A. Karthick, M.P.V. Jeyalekshmi, A.M.M.A.J. Decruz, A. M. Manokar, R. Sathyamurthy, Enhancing the fresh water produced from inclined cover stepped absorber solar still using wick and energy storage materials, Environ. Sci. Pollut. Res. 28 (14) (2021) 18146–18162.

[30] Z.M. Omara, A.E. Kabeel, M.M. Younes, Enhancing the stepped solar still performance using internal and external reflectors, Energy Convers. Manag. 78 (2014) 876–881.

[31] F.A. Essa, Z.M. Omara, A.S. Abdullah, S. Shanmugan, H. Panchal, A. Kabeel, R. Sathyamurthy, W.H. Alawee, A.M. Manokar, A.H. Elsheikh, Wall-suspended trays inside stepped distiller with Al2O3/paraffin wax mixture and vapor suction: experimental implementation, J.Energy Storage 32 (2020), 102008.

[32] A.M. Gandhi, S. Shanmugan, S. Gorjian, C.I. Pruncu, S. Sivakumar, A.H. Elsheikh, F.A. Essa, Z.M. Omara, H. Panchal, Performance enhancement of stepped basin solar still based on OSELM with traversal tree for higher energy adaptive control, Desalination 502 (2021), 114926.

[33] M.R. Diab, F.S. Abou-Taleb, F.A. Essa, Z.M. Omara, Improving the vertical solar distiller performance using rotating wick discs and integrated condenser, Environ. Sci. Pollut. Res. 29 (2022) 57946–57963.

[34] F.A. Essa, F.S. Abou-Taleb, M.R. Diab, Experimental investigation of vertical solar still with rotating discs, Energy Sources, Part A (2021) 1–21.

[35] M.R. Diab, F.S. Abou-Taleb, F.A. Essa, Effect of basin water depth on the performance of vertical discs' solar still—experimental investigation, Environ. Sci. Pollut. Res. (2022) 1–13.

[36] Z.S. Abdel-Rehim, A. Lasheen, Improving the performance of solar desalination systems, Renew. Energy 30 (13) (2005) 1955–1971.

[37] A.E. Kabeel, M.H. Hamed, Z.M. Omara, Augmentation of the basin type solar still using photovoltaic powered turbulence system, Desalin. Water Treat. 48 (1–3) (2012) 182–190.

[38] Z.M. Omara, A. Abdullah, T. Dakrory, Improving the productivity of solar still by using water fan and wind turbine, Sol. Energy 147 (2017) 181–188.

[39] A. Bamasag, F.A. Essa, Z. Omara, E. Bahgat, A.O. Alsaiari, H. Abulkhair, R. A. Alsulami, A.H. Elsheikh, Machine learning-based prediction and augmentation of dish solar distiller performance using an innovative convex stepped absorber and phase change material with nanoadditives, Process Saf. Environ. Prot. 162 (2022) 112–123.

[40] A. Abdullah, Z. Omara, H.B. Bacha, M. Younes, Employing convex shape absorber for enhancing the performance of solar still desalination system, J. Energy Storage 47 (2022), 103573.

[41] F.A. Essa, W.H. Alawee, S.A. Mohammed, H.A. Dhahad, A.S. Abdullah, Z. M. Omara, Experimental investigation of convex tubular solar still performance using wick and nanocomposites, Case Stud. Therm. Eng. 27 (2021), 101368.

[42] A.E. Kabeel, Z. Omara, F. Essa, Enhancement of modified solar still integrated with external condenser using nanofluids: an experimental approach, Energy Convers. Manag. 78 (2014) 493–498.

[43] S. Nazari, M. Bahiraei, H. Moayedi, H. Safarzadeh, A proper model to predict energy efficiency, exergy efficiency, and water productivity of a solar still via optimized neural network, J. Clean. Prod. 277 (2020), 123232.

[44] A. Kabeel, Z.M. Omara, F. Essa, A. Abdullah, T. Arunkumar, R. Sathyamurthy, Augmentation of a solar still distillate yield via absorber plate coated with black nanoparticles, Alex. Eng. J. 56 (4) (2017) 433–438.

[45] T. Arunkumar, D. Murugesan, K. Raj, D. Denkenberger, C. Viswanathan, D.D. W. Rufuss, R. Velraj, Effect of nano-coated CuO absorbers with PVA sponges in solar water desalting system, Appl. Therm. Eng. 148 (2019) 1416–1424.

[46] F.A. Essa, A.S. Abdullah, Z.M. Omara, Improving the performance of tubular solar still using rotating drum – experimental and theoretical investigation, Process Saf. Environ. Prot. 148 (2021) 579–589.

[47] A.S. Abdullah, W.H. Alawee, S.A. Mohammed, U.F. Alqsair, H.A. Dhahad, F. A. Essa, Z.M. Omara, Performance improvement of tubular solar still via tilting glass cylinder, nano-coating, and nano-PCM: experimental approach, Environ. Sci. Pollut. Res. 30 (2022) 1–12.

[48] F.A. Essa, A.S. Abdullah, Z.M. Omara, Rotating discs solar still: new mechanism of desalination, J. Clean. Prod. 275 (2020), 123200.

[49] M. Younes, A. Abdullah, Z. Omara, F. Essa, Enhancement of discs' solar still performance using thermal energy storage unit and reflectors: an experimental approach, Alex. Eng. J. 61 (10) (2022) 7477–7487.

[50] A.S. Abdullah, A. Alarjani, M.M. Abou Al-sood, Z.M. Omara, A.E. Kabeel, F.A. Essa, Rotating-wick solar still with mended evaporation technics: experimental approach, Alex. Eng. J. 58 (4) (2019) 1449–1459.

[51] A.S. Abdullah, Z.M. Omara, F.A. Essa, A. Alarjani, I.B. Mansir, M.I. Amro, Enhancing the solar still performance using reflectors and sliding-wick belt, Sol. Energy 214 (2021) 268–279.

[52] Z.M. Omara, A.S. Abdullah, F.A. Essa, M.M. Younes, Performance evaluation of a vertical rotating wick solar still, Process Saf. Environ. Prot. 148 (2021) 796–804.

[53] A.S. Abdullah, Z.M. Omara, A. Alarjani, F.A. Essa, Experimental investigation of a new design of drum solar still with reflectors under different conditions, Case Stud. Therm. Eng. 24 (2021), 100850.

[54] W.H. Alawee, S.A. Mohammed, H.A. Dhahad, A.S. Abdullah, Z.M. Omara, F. A. Essa, Improving the performance of pyramid solar still using rotating four cylinders and three electric heaters, Process Saf. Environ. Prot. 148 (2021) 950–958.

[55] A. Abdullah, M. Younes, Z. Omara, F. Essa, New design of trays solar still with enhanced evaporation methods–comprehensive study, Sol. Energy 203 (2020) 164–174.

[56] F.A. Essa, A.S. Abdullah, Z.M. Omara, A.E. Kabeel, Y. Gamiel, Experimental study on the performance of trays solar still with cracks and reflectors, Appl. Therm. Eng. 188 (2021), 116652.

[57] A.S. Abdullah, Z.M. Omara, F.A. Essa, M.M. Younes, S. Shanmugan, M. Abdelgaied, M.I. Amro, A.E. Kabeel, W.M. Farouk, Improving the performance of trays solar still using wick corrugated absorber, nano-enhanced phase change material and photovoltaics-powered heaters, J.Energy Storage 40 (2021), 102782.

[58] A. Abdullah, Z. Omara, F.A. Essa, U.F. Alqsair, M. Aljaghtham, I.B. Mansir, S. Shanmugan, W.H. Alawee, Enhancing trays solar still performance using wick finned absorber, nano-enhanced PCM, Alex. Eng. J. 61 (12) (2022) 12417–12430.

[59] F.A. Essa, Thermal Desalination Systems: From Traditionality to Modernity and Development, IntechOpen, London, 2022.

[60] M. Alsehli, F.A. Essa, Z. Omara, M.M. Othman, A.H. Elsheikh, M. Alwetaishi, S. Alghamdi, B. Saleh, Improving the performance of a hybrid solar desalination system under various operating conditions, Process Saf. Environ. Prot. 162 (2022) 706–720.

[61] H.E. Gad, S.M. El-Gayar, H.E. Gad, Performance of a solar still with clothes moving wick, in: Fifteenth International Water Technology Conference, IWTC, Alexandria, Egypt, 2011.

[62] Z. Haddad, A. Chaker, A. Rahmani, Improving the basin type solar still performances using a vertical rotating wick, Desalination 418 (2017) 71–78.

[63] G.M. Ayoub, L. Malaeb, P.E. Saikaly, Critical variables in the performance of a productivity-enhanced solar still, Sol. Energy 98 (2013) 472–484.

[64] L. Malaeb, K. Aboughali, G.M. Ayoub, Modeling of a modified solar still system with enhanced productivity, Sol. Energy 125 (2016) 360–372.

[65] A.S. Abdullah, F.A. Essa, Z.M. Omara, Y. Rashid, L. Hadj-Taieb, G.B. Abdelaziz, A. E. Kabeel, Rotating-drum solar still with enhanced evaporation and condensation techniques: comprehensive study, Energy Convers. Manag. 199 (2019).

[66] A. Elbrashy, F. Aboutaleb, M. El-Fakharany, F.A. Essa, Experimental study of solar air heater performance with evacuated tubes connected in series and involving nano-copper oxide/paraffin wax as thermal storage enhancer, Environ. Sci. Pollut. Res. (2022) 1–14.

[67] A. Elbrashy, F.S. Abou-Taleb, M.K. El-Fakharany, F.A. Essa, Experimental study of solar air heater performance by evacuated tubes connected in series and loaded with thermal storage material, J. Energy Storage 54 (2022), 105266.

[68] S. Bazri, I.A. Badruddin, M.S. Naghavi, M. Bahiraei, A review of numerical studies on solar collectors integrated with latent heat storage systems employing fins or nanoparticles, Renew. Energy 118 (2018) 761–778.

[69] A.E. Kabeel, K. Harby, M. Abdelgaied, A. Eisa, Augmentation of a developed tubular solar still productivity using hybrid storage medium and CPC: an experimental approach, J. Energy Storage 28 (2020), 101203.

[70] V.S. Vigneswaran, G. Kumaresan, B.V. Dinakar, K.K. Kamal, R. Velraj, Augmenting the productivity of solar still using multiple PCMs as heat energy storage, J. Energy Storage 26 (2019), 101019.

[71] V.P. Katekar, S.S. Deshmukh, A review of the use of phase change materials on performance of solar stills, J. Energy Storage 30 (2020), 101398.

[72] L. Sahota, G. Tiwari, Effect of nanofluids on the performance of passive double slope solar still: a comparative study using characteristic curve, Desalination 388 (2016) 9–21.

[73] A.S. Abdullah, F.A. Essa, H.B. Bacha, Z.M. Omara, Improving the trays solar still performance using reflectors and phase change material with nanoparticles, J. Energy Storage 31 (2020), 101744.

[74] U.F. Alqsair, A. Abdullah, Z. Omara, Enhancement the productivity of drum solar still utilizing parabolic solar concentrator, phase change material and nanoparticles' coating, J. Energy Storage 55 (2022), 105477.

[75] J. Holman, Experimental Methods for Engineers, Eighth ed., McGraw-Hill Companies, New York, 2012.

[76] A. Sarı, A. Karaipekli, Thermal conductivity and latent heat thermal energy storage characteristics of paraffin/expanded graphite composite as phase change material, Appl. Therm. Eng. 27 (8–9) (2007) 1271–1277.

[77] M. Younes, A. Abdullah, F. Essa, Z. Omara, M. Amro, Enhancing the wick solar still performance using half barrel and corrugated absorbers, Process Saf. Environ. Prot. 150 (2021) 440–452.

[78] F.A. Essa, A.S. Abdullah, W.H. Alawee, A. Alarjani, U.F. Alqsair, S. Shanmugan, Z. M. Omara, M.M. Younes, Experimental enhancement of tubular solar still performance using rotating cylinder, nanoparticles' coating, parabolic solar concentrator, and phase change material, Case Stud. Therm. Eng. 29 (2022), 101705.

[79] A.E. Kabeel, Z.M. Omara, F.A. Essa, Numerical investigation of modified solar still using nanofluids and external condenser, J. Taiwan Inst. Chem. Eng. 75 (2017) 77–86.

[80] F.A. Essa, W.H. Alawee, S.A. Mohammed, A.S. Abdullah, Z.M. Omara, Enhancement of pyramid solar distiller performance using reflectors, cooling cycle, and dangled cords of wicks, Desalination 506 (2021), 115019.

[81] S.A. Mousavi, M. Mehrpooya, A comprehensive exergy-based evaluation on cascade absorption-compression refrigeration system for low temperature applications-exergy, exergoeconomic, and exergoenvironmental assessments, J. Clean. Prod. 246 (2020), 119005.

[82] S.M. Parsa, A. Rahbar, D. Javadi, M. Koleini, M. Afrand, M. Amidpour, Energy-matrices, exergy, economic, environmental, exergoeconomic, enviroeconomic, and heat transfer (6E/HT) analysis of two passive/active solar still water desalination nearly 4000m: altitude concept, J. Clean. Prod. 261 (2020), 121243.